Supercluster of Electrons in Ultrathin TaSe$_2$ Nanocrystals

Takeshi Toshima, Katsuhiko Inagaki, Noriyuki Hatakenaka[1] and Satoshi Tanda

Department of Applied Physics, Hokkaido University, Sapporo 060-8628
[1]*Faculty of Intergrated Arts and Sciences, Hiroshima University, Higashi-Hiroshima, Hiroshima 739-8521*

We discover a supercluster of electrons in the ultrathin TaSe$_2$ crystals synthesized by our developed de-chalcogenide method. The supercluster has an unexpected structure containing 61 electrons denoted by $\sqrt{61} \times \sqrt{61}$, in addition to a $\sqrt{49} \times \sqrt{49}$ supercluster based on $\sqrt{7} \times \sqrt{7}$ clusters expected in triangle lattices. This new hierarchal structure and successive clustering cannot be explained by a conventional electron clustering mechanism assisted by background lattice distortions, i.e., charge-density-wave formation mechanism based on Fermi surface nesting. We propose an alternative possible formation mechanism based on saddle-point nesting, taking into account a trigonal symmetry as well as lattice distortion energy.

1. Introduction

Successive clustering leads to supercluster with hierarchy,[1] i.e., a cluster of clusters, found in various systems ranging from supermolecule dendrimers,[2] icosahedral packing of B$_{12}$[3,4] to supergalaxy.[5] Clustering as a building block of supercluster needs an attractive force like gravitation in supergalaxy, while a repulsive force does not promote clustering. In fact, electrons governed by Coulomb repulsion only form a homogeneous trigonal lattice known as Wigner crystal.[6,7] In crystals, an attractive force between electrons is introduced by the electron–phonon interaction. At lower (one or two) dimensions, electric instability occurs due to an electron–phonon interaction related to Fermi surface nesting characterized by the Fermi wave vector kF. This leads to a new type of condensed phase called a charge density wave (CDW)[8–10] where the conduction electron density is modulated like a wave, and the lattices are simultaneously modulated from their original positions, resulting in a kind of electron's cluster. 1T–TaSe$_2$ is a typical two-dimensional CDW material with a width and length of 0.1–10 mm and a thickness of 10–100 μm, and which is usually synthesized by the chemical vapour transport method.[11] The resulting structure is a $\sqrt{13} \times \sqrt{13}$ cluster containing 13 electrons[12] as shown in Fig. 1. However, it appears to be difficult for a thick system to form a cluster of clusters, i.e., an electrons supergalaxy in solids because of crystal rigidity. Thinner systems with flexibility are required for the creation of a supercluster.

2. Experimental

We develop a new method to enhance two dimensionality of the system by making a thinner film using the "de-chalcogenide method". The starting material is TaSe$_3$ fibre, which is used as a template. The TaSe$_3$ crystals are synthesized by the conventional chemical vapour transport method. The size of the TaSe$_3$ crystals is typically 10 nm–1 mm (thickness and width) and 100 nm–1 cm (length). We convert the TaSe$_3$ crystals with nanoscale to TaSe$_2$ ultrathin films. The TaSe$_3$ crystals are set on a quartz plate in a sample chamber (Thermo Riko IVF298) evacuated to about 1×10^{-5} Torr. The sample chamber at approximately $1 \times$ 10^{-3} Torr is filled with hydrogen gas in order to remove the oxygen gas. The TaSe$_3$ crystals are heated rapidly from room temperature to 600 K and then reacted with hydrogen gas for about 30 min. The chemical reaction is expressed as TaSe$_3$ + H$_2$(gas) → TaSe$_2$ + H$_2$Se(gas). One selenium atom is removed from the TaSe$_3$ template per unit cell (TaSe$_3$ → TaSe$_2$ + Se), resulting in the growth of a TaSe$_2$ thin film on the surface of TaSe$_3$ fibre as shown in Fig. 2(f). The surface TaSe$_3$ crystal is converted into a TaSe$_2$ monolayer near the surface during the de-chalcogenide processes [from Figs. 2(a) to 2(b)]. These obtained crystals are suspended in isopropyl alcohol by sonic dispersion of 30 min to strip ultrathin TaSe$_2$ film from TaSe$_3$ surface. The size of the TaSe$_2$ crystals is typically 10 nm–10 μm (width and length) and 10 nm (thickness). Submicron TaSe$_2$ crystals are deposited on a substrate. We analyze these crystals by their transmission electron diffraction (TED) pattern.

3. Experimental Result and Discussion

Figure 3(a) shows the TED pattern of the TaSe$_2$ thin film. From the Bragg refraction and satellite spots, the crystal is a hexagonal structure with lattice constants $a = b = 3.49$ Å (± 0.03 Å) modulated by a CDW characterized by the CDW wave vectors, $Q_1 = (0.286 \pm 0.002)a^* + (0.143 \pm 0.002)b^*$, $Q_2 = (-0.142 \pm 0.002)a^* + (0.425 \pm 0.002)b^*$, and $|Q| = 0.378(\pm 0.005 \text{ Å}^{-1})$. Figure 3(b), which is a Fourier transformation of Fig. 3(a), shows real-space images of the crystal. Figure 3(b) clearly shows different translational vectors with $\sqrt{7}$ times the lattice constant in contrast to the trigonal vectors. This crystal is then identified as a $\sqrt{7} \times \sqrt{7}$ CDW structure involving seven atoms, a centre atom (bold black spot) surrounded by six atoms (faint spots), in the unit cell as shown in Fig. 4(b). The same structure has been reported in an intercalated system.[13]

Figure 3(c) shows TED patterns of the crystal shown in Fig. 3(a) obtained from an adjacent location. This reveals the existence of an unprecedented CDW structure with the same lattice constants $a = b = 3.42$ Å (± 0.005 Å). Figure 3(d), which is a Fourier transformation of Fig. 3(c), characterizes the CDW structure by using conventional CDW wave vectors, $Q_1 = (0.064 \pm 0.002)a^* + (0.082 \pm 0.002)b^*$, $Q_2 = (-0.146 \pm 0.002)a^* + (0.065 \pm 0.002)b^*$,
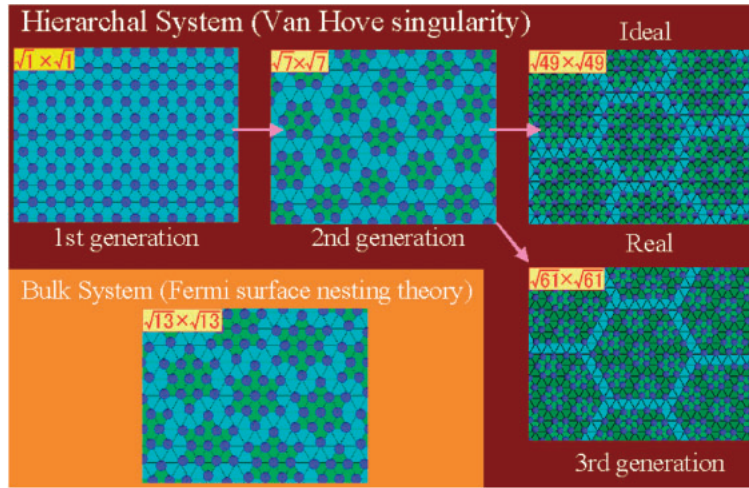
Fig. 1.   A model of clustering in a two-dimensional trigonal system. The blue spheres are atoms or electrons. In a bulk system, an attractive force compels the system to form a cluster only once due to Fermi instability when the attractive force caused by Fermi surface nesting is stronger than the force caused by the Van Hove singularity. For example, the system shows a $\sqrt{13} \times \sqrt{13}$ CDW phase. In thinner systems, the attractive force caused by the Van Hove singularity could be stronger than the force caused by Fermi surface nesting. The first generation shows no atom modulation. In the second generation, a centre atom attracts six neighbouring atoms. The clusters form a trigonal lattice again. In an ideal third generation, the centre cluster attracts six neighbouring clusters. With the real third generation, however, a centre cluster attracts six neighbouring clusters where 12 atoms lie on the vertex of a hexagonal supercluster and act like a cushion.
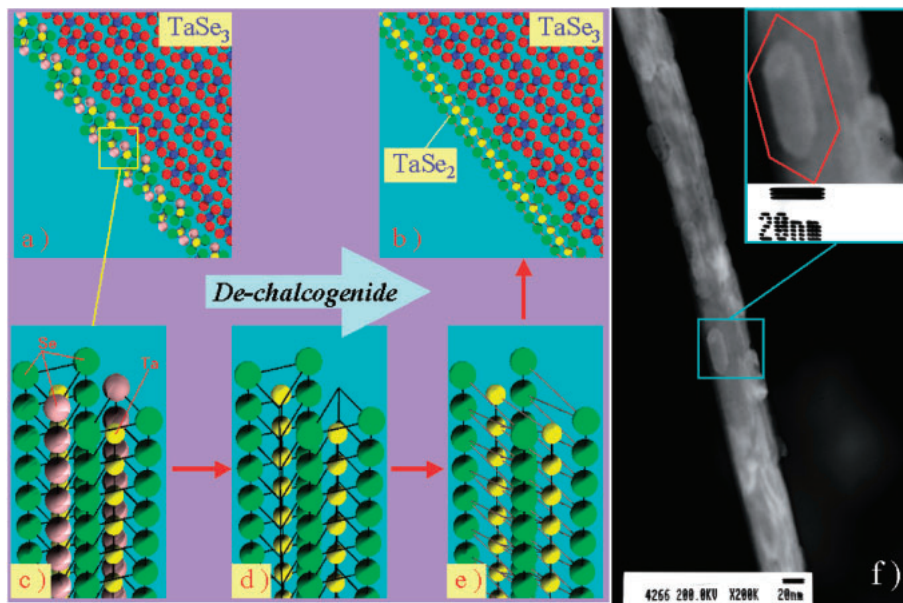
Fig. 2.   A schematic diagram of de-chalcogenide processes. The TaSe$_2$ crystal is synthesized from TaSe$_3$ crystal in the sequence (a)–(c)–(d)–(e)–(b). In (a), the TaSe$_3$ crystal starting material is shown by the b-axis. The red, green, and pink spheres represent selenium atoms and the blue and yellow spheres are tantalum atoms. (c), (d), and (e) are enlarged views of the square yellow area in (a). Selenium atoms belonging to the TaSe$_3$ surface (pink spheres) are removed [(c) to (d)], and then new dangling bonds form in the removed area. The dangling bonds immediately vanish owing to their highly reactive properties by combining with the neighbouring TaSe$_3$ [(d) to (e)]. Finally the surface TaSe$_3$ crystal becomes TaSe$_2$ crystal [(e) to (b)]. (f) is a transmission electron microscope (TEM) image of TaSe$_2$ crystals growing on the TaSe$_3$ crystal. Inset is an enlarged image of the blue-squared area. The needle-like structure is TaSe$_3$, which is the mother material, and the hexagonal crystal attached to the needle crystal is TaSe$_2$ thin crystal.

and $|Q| = 0.12$ ($\pm 0.01 \, \text{Å}^{-1}$) or, $\boldsymbol{R} = 5\boldsymbol{a} + 4\boldsymbol{b}$ and $|\boldsymbol{R}|$ is $\sqrt{61}$ times the lattice constant. Thus the new CDW crystal is identified as a $\sqrt{61} \times \sqrt{61}$ CDW structure. In addition, the new $\sqrt{61} \times \sqrt{61}$ CDW is constructed from $\sqrt{7} \times \sqrt{7}$ CDW clusters as shown in the inset of Fig. 3(d). Therefore this $\sqrt{61} \times \sqrt{61}$ CDW is a supercluster.

Let us consider the supercluster formation mechanism. 1T–TaSe$_2$ crystal ordinarily forms a $\sqrt{13} \times \sqrt{13}$ CDW structure (13 electron cluster) as a result of Fermi instability.[12] In contrast, the observed $\sqrt{61} \times \sqrt{61}$ superstructure

is not explained by conventional CDW nesting theory because there is no possibility of a phase transition. The attractive force required for clustering acts only once when the system has undergone a CDW transition. Therefore, we have to find an alternative superclustering mechanism.

We employ the CDW theory proposed by Rice and Scott[14] to account for the hierarchal structure we discovered. According to their theory, electrons may form a CDW structure without reference to Fermi surface nesting 2kF if an electron density of states has saddle points in its band
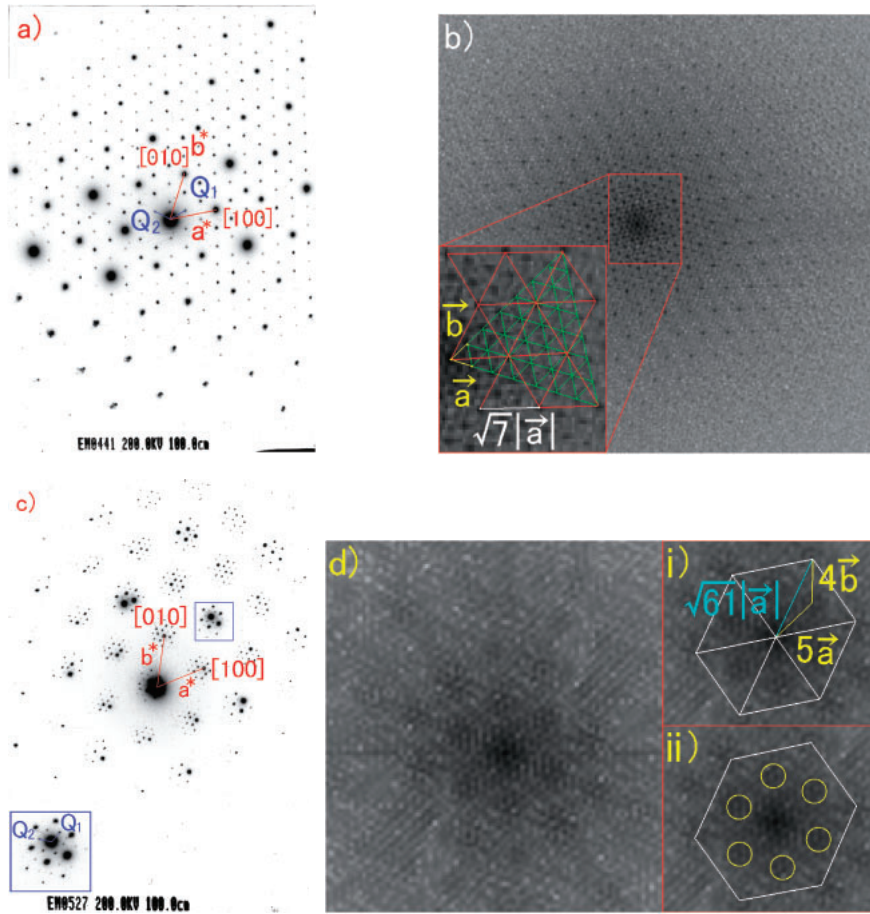
Fig. 3. (a) and (c) are TED images of a TaSe$_2$ thin film. (b) and (d) are fast Fourier transform (FFT) images of (a) and (c), respectively. The bold black spot in (a), are caused by the Bragg reflection of TaSe$_2$, a^* and b^* are reciprocal lattice vectors. The faint spots around the bold black spot are satellites resulting from $\sqrt{7} \times \sqrt{7}$ CDW modulation. Q_1 and Q_2 are CDW wave vectors. The inset FFT image (b) is an enlarged image of the area outlined with a red square. The spots show the tantalum atom positions. The distance between neighbouring spots corresponds to the lattice constant indicated in the inset as a and b. The distance between bold black spots is $\sqrt{7} \times |a|$, reflecting the $\sqrt{7} \times \sqrt{7}$ CDW structure. (c) is TED image of TaSe$_2$ with a $\sqrt{61} \times \sqrt{61}$ CDW state. The inset is an enlarged image of the area outlined with a blue square. We observed CDW wave vectors Q_1 and Q_2 as well as the reciprocal lattice vectors a^* and b^*. The inset in FFT image (d) is an enlarged image of the centre. A new translational vector described by the vector $R = 5a + 4b$ is observed. Moreover, an internal structure is also discovered in the unit of the $\sqrt{61} \times |a|$ structure.
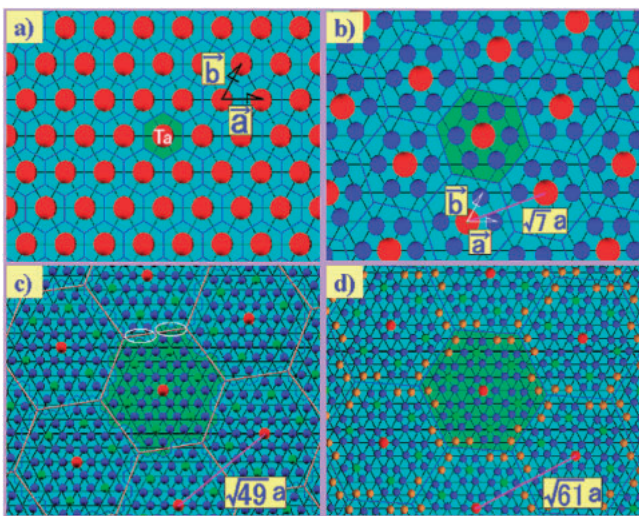
Fig. 4. A model of the hierarchal structure in the two-dimensional trigonal TaSe$_2$ system. The coloured spheres are tantalum atoms. The black lines show the basic trigonal lattice. Vectors a and b are translational vectors of TaSe$_2$. (a) is the first generation without the CDW state. The basic unit has one atom and occupies the green hexagonal area. The centre atoms are represented by the vector $R_1 = a$. (b) is the second generation with a $\sqrt{7} \times \sqrt{7}$ CDW state. The cluster has seven atoms (one red and six blue atoms) and occupies the green hexagonal area. The centre atoms are expressed by the vector $R_2 = 2a + b$. (c) is the ideal third generation with the $\sqrt{49} \times \sqrt{49}$ CDW state. The supercluster has seven second-generation clusters and occupies the green non-smooth area. The centre atoms are combined for the vector $r = 5a + 3b$. If we draw a smooth hexagonal boundary such as the pink line, the areas outlined with white circles act as load positions. (d) is an observed third generation with the $\sqrt{61} \times \sqrt{61}$ CDW state. The supercluster includes a $\sqrt{49} \times \sqrt{49}$ structure and twelve atoms (gold spheres), and occupies the smooth hexagonal green area. The distance between red spheres is $\sqrt{61} \times |a|$. The centre atoms are combined for the vector $R_3 = 5a + 4b$.

structure. At the saddle points, a large number of electrons resulting from the Van Hove singularity[15] contribute to the scattering processes, resulting in the same electric instability. We consider that the first generation hierarchal structure is a non-CDW structure, where electrons form a

trigonal structure on a two-dimensional system, as shown in Fig. 4(a). Studies of Wigner crystals have shown that two-dimensional trigonal electron systems have saddle points.[16] Note that 2H–TaSe$_2$ crystals also have saddle points.[17] Such the saddle points can also cause CDW formation.[14,17] We

Table I. Clustering number and coordinate. α_n mean number of atoms belonging to each generation of cluster. A_n and B_n mean coordinate of an atom position of neighbor cluster. Supercluster vector is a vector between centre atom of a cluster and centre atom of neighbor cluster. (Show in Fig. 4)

Generations	α_n	(A_n, B_n)	Supercluster vector
First generation	1	(1, 0)	$\boldsymbol{R}_1 = \boldsymbol{a}$ [Fig. 4(a)]
Second generation	7	(2, 1)	$\boldsymbol{R}_2 = 2\boldsymbol{a} + \boldsymbol{b}$ [Fig. 4(b)]
Third generation	61	(5, 4)	$\boldsymbol{R}_3 = 5\boldsymbol{a} + 4\boldsymbol{b}$ [Fig. 4(c)]
Fourth generation	547	(14, 13)	$\boldsymbol{R}_4 = 14\boldsymbol{a} + 13\boldsymbol{b}$
Nth generation	$\dfrac{3^{2n-1} + 1}{4}$	$\left(\dfrac{3^{n-1} + 1}{2}, \dfrac{3^{n-1} - 1}{2}\right)$	$\boldsymbol{R}_n = A_n\boldsymbol{a} + B_n\boldsymbol{b}$

assume that saddle points promote the formation of a $\sqrt{7} \times \sqrt{7}$ CDW structure, in which an atom (electron) attracts six atoms (electrons) around it, as shown in Fig. 4(b). This is reminiscent of the $\sqrt{7} \times \sqrt{7}$ CDW structure in a quantum Hall liquid system with a weak external magnetic field.[18] However, nesting vector between the saddle points on Γ–J line[16,17] does not coincide with the wave vectors of $\sqrt{7} \times \sqrt{7}$ CDW we discovered. The position of saddle points probably does not lie on Γ–J line due to difference of crystal structure between 1T–TaSe$_2$ and 2H–TaSe$_2$, the size of crystals and possibility of expansion of distance between layers.[13]

There is an advantage in the assumption of the saddle points. One free electron remains in the resulting cluster of the $\sqrt{7} \times \sqrt{7}$ CDW structure, as described in a previous report on the $\sqrt{13} \times \sqrt{13}$ CDW structure.[19] The excess electrons again form a trigonal lattice with $\sqrt{7}$ times the first generation. If such excess electrons form new saddle points as with the first generation, the resulting cluster will attract six neighbouring clusters. The supercluster again has seven clusters and one free electron regardless of the crystal structure, as shown in Fig. 4(c). A cluster of superclusters would be produced by the same rule. This model can account for the observed hierarchal structure. The next stable cluster is therefore expected to be a $\sqrt{49} \times \sqrt{49}$ supercluster, where a cluster (electron) attracts six clusters (electrons) around it. However, our result shows that the $\sqrt{61} \times \sqrt{61}$ supercluster includes a $\sqrt{49} \times \sqrt{49}$ supercluster based on $\sqrt{7} \times \sqrt{7}$ clusters. In other words, twelve extra Ta atoms are attached to the $\sqrt{49} \times \sqrt{49}$ supercluster in the third generation as shown in Fig. 4(d). This is due to the energy relaxation of the lattice displacement at the boundaries of the $\sqrt{49} \times \sqrt{49}$ supercluster structure as shown in Fig. 4(c). Note that the boundary of the $\sqrt{49} \times \sqrt{49}$ supercluster is rough where the strain energies are accumulated (white circled area). Twelve extra atoms are necessary to smooth the boundary. The actual third generation is then a $\sqrt{61} \times \sqrt{61}$ CDW structure, as shown in Fig. 4(d).

Our supercluster on a two-dimensional trigonal system is summarized by introducing a clustering number α_n and coordinate (A_n, B_n) where n stands for generation in a hierarchy (Table I). The clustering number α_n is the number of atoms or electrons that belong to each unit cell expressed as

$$\alpha_n = 7 \times \alpha_{n-1} + (6/3) \times (\alpha_{n-1} - 1) = 9 \times \alpha_{n-1} - 2, \quad (1)$$

where $\alpha_1 = 1$. The formula consists of a "hierarchal" term and a "relaxation" term. The prior unit attracts the six neighbouring units and forms a new unit. With trigonal symmetry, there are seven atoms in the hierarchal term. If there is only the first term, $\alpha_n = 7^{n-1}$ is written with the usual simple fractal formula.[20] The second term is due to the background, and the lattice deformation energy acts as the crack. The factor 6/3 means that each cluster shares six load points that lie on their vertexes with three neighbouring clusters in Fig. 4(d). Formula (1) is reduced to a simple formula

$$\alpha_n = \frac{3^{2n-1} + 1}{4}. \quad (2)$$

The clustering coordinate specifies the centre position of each cluster using a translation vector, $\boldsymbol{R}_n = A_n \times \boldsymbol{a} + B_n \times \boldsymbol{b}$, of the trigonal lattice system $\boldsymbol{a}$ and $\boldsymbol{b}$ as shown in Fig. 4(a). The clustering coordinate is then written as

$$(A_n, B_n) = \left(\frac{3^{n-1} + 1}{2}, \frac{3^{n-1} - 1}{2}\right). \quad (3)$$

According to this formula, the fourth generation is expected to be a $\sqrt{547} \times \sqrt{547}$ structure with $\boldsymbol{R}_4 = 14\boldsymbol{a} + 13\boldsymbol{b}$. The hierarchal structures led by the formula are different from a simple fractal structure such as a Koch curve or a Sierpinski gasket, but resemble a natural network such as the distribution of sunflower seeds, the texture of a snail shell or a honeycomb. The shape of the boundary between the clusters distinguishes these hierarchal structures. The concept of relaxation, namely smoothing, leads us to consider another hierarchal structure.

4. Conclusion

We have synthesized the nanoscale TaSe$_2$ crystals by our developed de-chalcogenide method using the template of TaSe$_3$ nanofibre. We also observed the crystals by transmission electron microscope image and diffraction analysis. The electrons on such the thin crystals form $\sqrt{7} \times \sqrt{7}$ and $\sqrt{61} \times \sqrt{61}$ CDW structure. The $\sqrt{61} \times \sqrt{61}$ structure has another periodicity inner; this result shows hierarchal supercluster of electrons clusters is realized. Conventional CDW mechanism of Fermi surface nesting dose not promote such the hierarchal structure, we apply the saddle-point nesting mechanism to explain the origin of hierarchy. Once trigonal system forms $\sqrt{7} \times \sqrt{7}$ structure due to saddle-point nesting, new system also becomes the trigonal system with $\sqrt{7}$ times scale and new saddle points also born. From these results, we introduce a clustering number and coordinate of trigonal system. Further studies both experimental and theoretical of other superclustering systems will unveil the principle of the clustering mechanism.

Acknowledgment

1) B. B. Mandelbrot: *The Fractal Geometry of Nature* (W. H. Freeman and Company, New York, 1982).
2) D. A. Tomalia, H. Baker, J. Dewald, M. Hall, G. Kallos, S. Martin, J. Roeck, J. Ryder and P. Smith: Polym. J. **17** (1985) 117.
3) A. Mackey: Nature **391** (1998) 334.
4) H. Hubert, B. Devouard, L. A. J. Garvie, M. O'Keeffe, P. R. Buseck, W. T. Petuskey and P. F. McMillan: Nature **391** (1998) 376.
5) V. de Lapparent, M. J. Geller and J. P. Huchra: Astronom. J. Lett. **302** (1986) 1.
6) E. P. Wigner: Phys. Rev. **46** (1934) 1002.
7) C. C. Grimes and G. Adams: Phys. Rev. Lett. **42** (1979) 795.
8) J. A. Wilson, F. J. DiSalvo and S. Mahajan: Phys. Rev. Lett. **32** (1974) 882.
9) R. E. Peierls: *Quantum Theory of Solids* (Clarendon Press, Oxford, 1955).
10) G. Grüner: *Density Waves in Solids* (Addison-Wesley, Massachusetts, 1994).
11) H. Schafer: *Chemical Transport Reactions* (Academic Press, New York, 1964).
12) F. J. DiSalvo, J. A. Wilson, B. G. Bagley and J. V. Waszczak: Phys. Rev. B **12** (1975) 2220.
13) G. J. Tatlock and J. V. Acrivos: Philos. Mag. **38** (1978) 81.
14) T. M. Rice and G. K. Scott: Phys. Rev. Lett. **35** (1975) 120.
15) L. Van Hove: Phys. Rev. **89** (1953) 1189.
16) X. Wan and R. N. Bhatt: Phys. Rev. B **65** (2002) 233209.
17) R. Liu, C. G. Olson, W. C. Tonjes and R. F. Frindt: Phys. Rev. Lett. **80** (1998) 5762.
18) A. A. Koulakov, M. M. Fogler and B. I. Shklovskii: Phys. Rev. Lett. **76** (1996) 499.
19) P. Fazekas and E. Tosatti: Philos. Mag. B **39** (1979) 229.
20) A. D. Stoycheva and S. J. Singer: Phys. Rev. E **65** (2002) 036706.